

AD-A219 127

(4)

DTIC FILE COPY

Technical Document 1685
November 1989

**Specification for
Environmental
Measurements to
Assess Radar
Sensors**

Richard A. Paulus

DTIC
111330
8

Approved for public release; distribution is unlimited.

90 03 09 078

NAVAL OCEAN SYSTEMS CENTER

San Diego, California 92152-5000

J. D. FONTANA, CAPT, USN
Commander

R. M. HILLYER
Technical Director

ADMINISTRATIVE INFORMATION

Funding was provided by the Naval Sea Systems Command.

Released by
H. V. Hitney, Head
Tropospheric Branch

Under authority of
J. H. Richter, Head
Ocean and Atmospheric
Sciences Division

ACKNOWLEDGMENTS

Reviewers of this document during its development were:

R. K. Cross (NDHQ/Ottawa, Canada); H. V. Hitney and W. L. Patterson (Naval Ocean Systems Center); W. P. M. N. Keizer (Physics and Electronics Laboratory TNO, The Netherlands); and J. P. Reilly (Johns Hopkins University Applied Physics Laboratory).

CONTENTS

| | | |
|------------|--|-----------|
| 1.0 | INTRODUCTION | 1 |
| 2.0 | MARINE ATMOSPHERIC BOUNDARY LAYER | 2 |
| 3.0 | UPPER AIR MEASUREMENTS | 3 |
| 3.1 | Refractive Structure | 3 |
| 3.2 | Measurements and Procedures | 6 |
| 4.0 | SURFACE MEASUREMENTS | 8 |
| 4.1 | Surface Layer | 8 |
| 4.1.1 | Refractive Structure | 8 |
| 4.1.2 | Measurements and Procedures | 12 |
| 4.1.2.1 | Wind Speed | 12 |
| 4.1.2.2 | Air Temperature and Relative Humidity | 13 |
| 4.1.2.3 | Sea Surface Temperature | 13 |
| 4.2 | Ocean Waves | 13 |
| 5.0 | EQUIPMENT REFERENCES | 15 |
| 6.0 | GLOSSARY | 16 |
| 7.0 | REFERENCES | 17 |

APPENDIXES:

| | | |
|-----------|--|------------|
| A. | Development of the Evaporation Duct Height Formulation | A-1 |
| B. | Critical Gradient of Potential Refractivity | B-1 |
| C. | Implementing a Modified Evaporation Duct Height Calculation | C-1 |
| D. | FORTRAN Program to Calculate Evaporation Duct Height | D-1 |
| E. | Test Cases for Evaporation Duct Height Calculation | E-1 |
| F. | M-Profiles in the Surface Layer | F-1 |

| | |
|--------------------|-------------------------------------|
| Accession For | |
| MRG | <input checked="" type="checkbox"/> |
| DRG | <input checked="" type="checkbox"/> |
| Un | <input type="checkbox"/> |
| Justification | |
| By | |
| Distribution/ | |
| Availability Codes | |
| Dist | Special |
| A-1 | |

1.0 INTRODUCTION

The purpose of this document is to prescribe the minimum requirements for measuring environmental parameters that affect the evaluation of proposed radar systems. These environmental factors must be properly measured to ensure fair appraisals of competing designs and to assess expected long-term performance. The procedures for short-term in-situ measurements pertinent to microwave propagation and sea clutter are addressed in sections 2.0 through 4.0. Measurement accuracies are specified and several types of instruments are discussed in these sections. Specific manufacturers and retailers are mentioned as sources for various types of instruments and equipment in section 5.0. This listing is not all-inclusive and is not intended to be an endorsement of those companies or products. Section 6.0 is a glossary of terms used in instrument specifications. Appendixes A through F are included as background material for determining refractive structure from surface meteorological measurements. (KR) ←

Environmental measurements relevant to clutter from clouds, rain, land, birds, and insects are not addressed. Environmental measurement specifications relevant to the performance of infrared systems are set forth in a separate NATO Anti-Air Warfare System (NAAWS) document.

Previous work performed under the NAAWS project has shown that certain environmental factors strongly affect overall radar system performance. For shipborne radars operating at frequencies above L-band, the evaporation duct is the dominant propagation mechanism affecting the maximum detection range of horizon-search radars.¹ In addition, surface-based ducts may also affect the detection capabilities of horizon-search radars. Ducting can also increase sea clutter return within and beyond the normal horizon, and surface-based ducts can enhance land clutter return from greatly extended ranges.² Sea clutter return is also dependent upon sea state, which in turn is dependent upon wind speed, wind direction, fetch, and duration.

2.0 MARINE ATMOSPHERIC BOUNDARY LAYER

The marine atmospheric boundary layer is the coupling region between the free atmosphere and the ocean. Air-sea interaction effects occur at the bottom of the boundary layer, within the surface layer, with the transport of momentum, heat, and moisture. The surface layer is a few tens of meters thick. Above the surface layer, buoyant and mechanical turbulence tend to yield a well-mixed layer within which gradients of meteorological parameters are constant. The thickness of the mixed layer varies from a few hundred to a thousand meters. Often, the mixed layer is capped by an interfacial layer that provides a transition between the mixed layer and the free atmosphere. The interfacial layer may be quite weak or even nonexistent. If it is present, this layer is characterized by an increase in temperature and a decrease in moisture. Idealized profiles of temperature and moisture in the boundary layer are shown in Fig. 1, which is adapted from Davidson *et al.*³

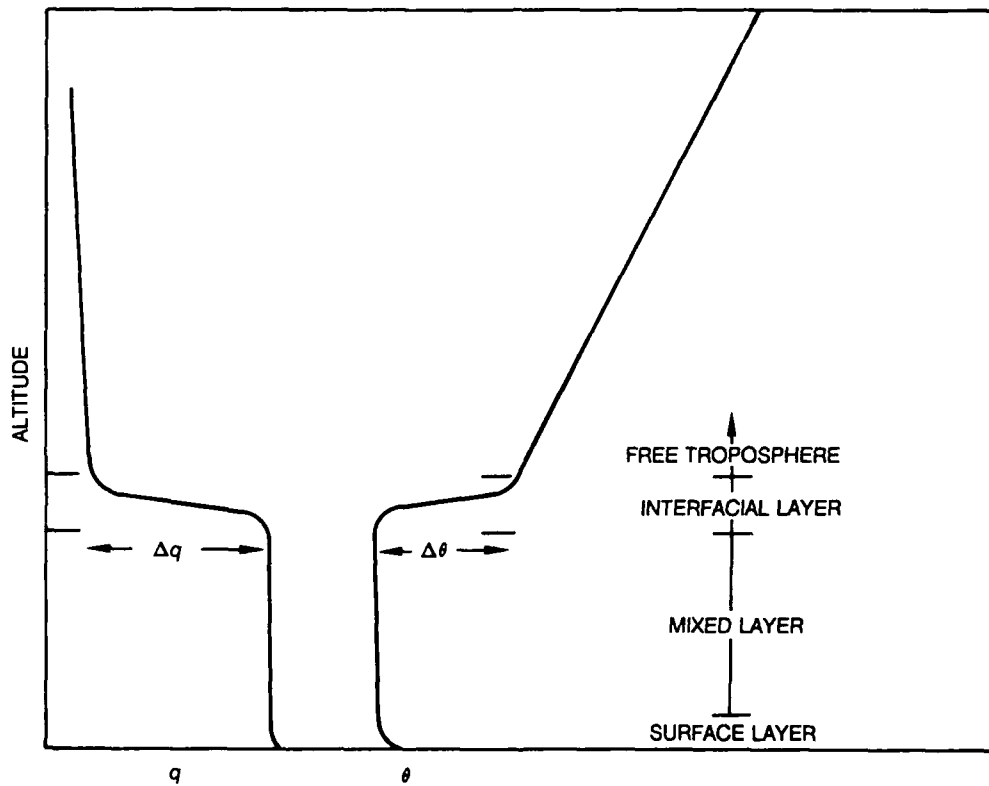


Figure 1. Idealized profiles of potential temperature, θ , and specific humidity, q , in a well-mixed boundary layer. (Adapted from Ref.3.)

3.0 UPPER AIR MEASUREMENTS

Measurements of the profiles of Fig. 1 in the mixed layer and above are usually done with a radiosonde carried aloft by a free balloon. The radiosonde measures pressure, temperature, and (usually) relative humidity as it ascends through the atmosphere and telemeters these data to a ground-station receiver. The output of the ground station may be either digital or analog. The analog data must be converted to engineering units of pressure (P in millibars), temperature (T in Celsius), and relative humidity (RH in percent). These data can then be converted to refractivity, N

$$N = \frac{77.6 P}{T} + 3.73 \times 10^5 \frac{e}{T^2}$$

or modified refractivity, M

$$M = N + 0.157 h$$

where P is pressure in millibars, T is temperature in Kelvin, e is water vapor pressure in millibars, and h is height in meters. The ambient water vapor pressure, e , is

$$e = e_s \frac{RH}{100}$$

where RH is relative humidity in percent and saturation water vapor pressure, e_s , in millibars, can be determined from

$$e_s = 6.105 \exp \left[25.22 \left(\frac{T - 273.2}{T} \right) - 5.31 \ln \frac{T}{273.2} \right]$$

where T is air temperature in Kelvin and \ln is the natural logarithm.

3.1 REFRACTIVE STRUCTURE

Refractive gradients have been qualitatively characterized by their effects. The standard atmosphere gradient determined from climatological data has been defined as 118 M/km . This gradient causes an electromagnetic wave to bend slightly toward the surface of the earth so that the radar horizon is slightly greater than the geometric horizon. Of course, this value varies with meteorological conditions; gradients different from 118 M/km that do not have dramatic effects on propagation are referred to as normal. Gradients less than normal cause electromagnetic waves to bend even more toward the earth's surface and are referred to as superrefractive. The extreme case of superrefraction is called trapping, when electromagnetic waves are bent downward with a curvature greater than that of the earth. The trapping layer thus forms a duct that can behave very much like a waveguide. Gradients much greater than 118 M/km are called subrefractive and result in electromagnetic waves being bent away from the earth's surface. Table 1 summarizes the refractive gradients.

Table 1. Relation of *N*- and *M*-gradients.

| Gradient Type | <i>N</i> -Gradient | <i>M</i> -Gradient |
|-----------------|------------------------------|----------------------------|
| Trapping | ≤ -157 <i>N</i> /km | ≤ 0 <i>M</i> /km |
| Superrefractive | -157 to -79 <i>N</i> /km | 0 to 79 <i>M</i> /km |
| Normal | -79 to 0 <i>N</i> /km | 79 to 157 <i>M</i> /km |
| Subrefractive | > 0 <i>N</i> /km | >157 <i>M</i> /km |

The temperature and moisture gradients in the interfacial layer usually result in a superrefractive layer. If the gradients in the interfacial layer are sufficiently strong, a trapping layer will be formed. If the trapping layer occurs well above the surface, an elevated duct will be formed (Fig. 2a). If the gradients in the interfacial layer are stronger, or the trapping layer occurs at a lower height, a surface-based duct will be formed (Fig. 2b). These two types of duct are formed under stable atmospheric conditions and vary slowly in range and time. Under unusual conditions, the interfacial layer may occur at the surface, creating a surface-based duct from a surface trapping layer (Fig. 2c). This situation typically occurs downwind of a large land mass and is often characterized by a strong variation of the refractive structure with range and time.

An elevated duct, whose base is more than a few hundred meters above the surface, will have little impact on surface-to-surface propagation. A surface-based duct from an elevated refractive layer will have little impact within the normal radar horizon but may provide detection capability and significant clutter return from well beyond the horizon. The surface-based duct from a surface trapping layer will be the dominant propagation mechanism when this condition exists. Radar propagation and clutter signals will be dependent upon the gradient and thickness of the trapping layer.

Although trapping layers and the associated ducts give rise to the most dramatic effects, superrefractive and subrefractive layers may also affect propagation and clutter. Craig *et al.* discuss these various meteorological effects in detail.⁴

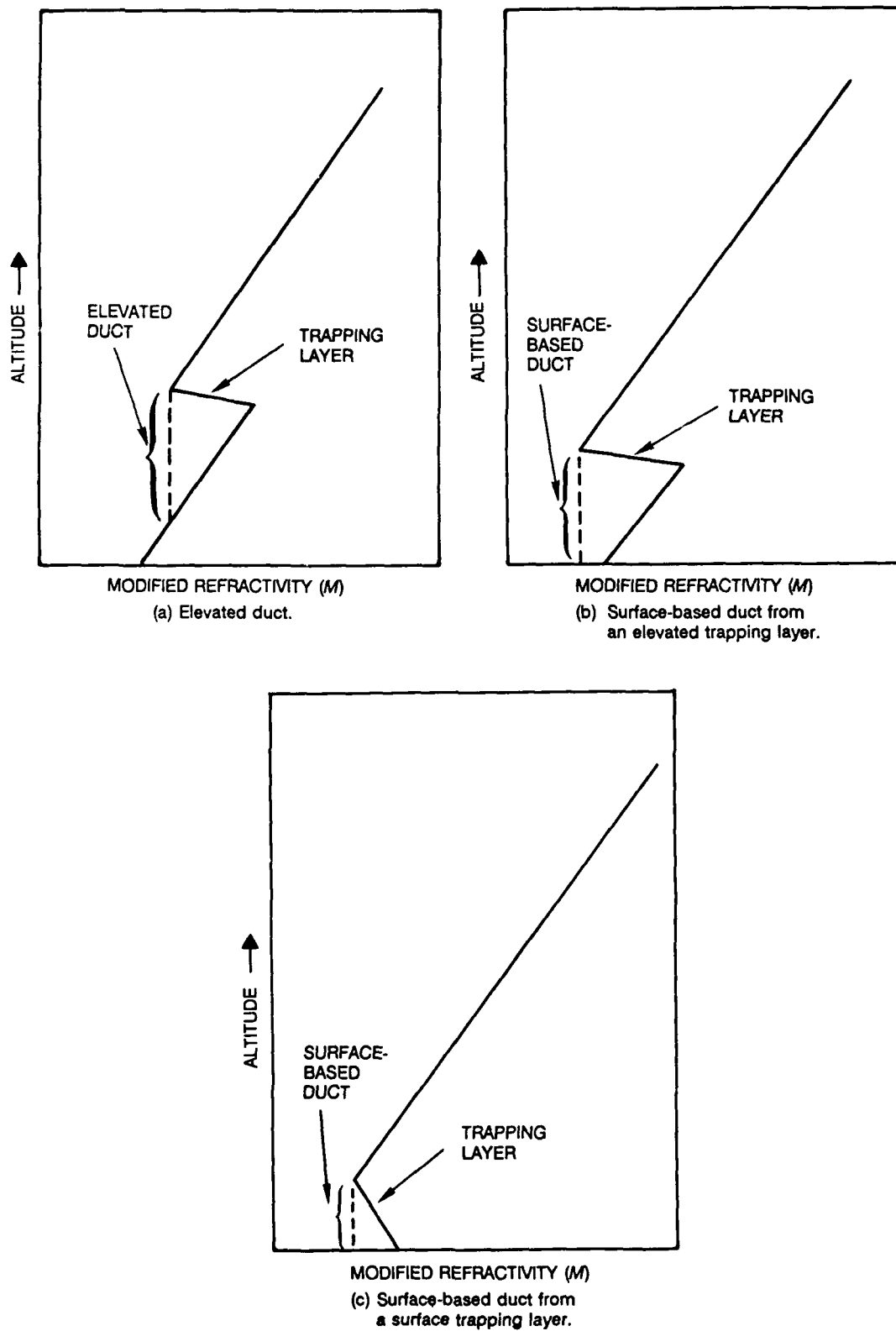


Figure 2. Idealized modified refractivity profiles.

3.2 MEASUREMENTS AND PROCEDURES

When the vertical profile of refractivity is being measured, the absolute accuracy of the data is not as important as an accurate measurement of the gradients. Sensor lag tends to reduce gradients and increase the altitudes at which the changes in gradient appear. The lag errors are not too serious at normal ascension rates but can be very significant in the first several tens of meters above the surface if the sensor has been abnormally heated or cooled just before launch.⁵ This mainly affects the radiosondes with carbon hygistor humidity elements, which have a relatively large thermal mass, but other types of humidity sensors and temperature sensors can also be affected by surface or platform heating. Careful preparation and handling of the instrument package before launch can minimize these problems.

Table 2 shows the minimum specifications for radiosonde sensors. For conditions typical of the NAAWS area of interest, these sensor specifications will nominally provide 1 to 2 *N*-units resolution as calculated from the root of the sum of the squares:

$$\Delta N = [(a\Delta P)^2 + (b\Delta T)^2 + (c\Delta RH)^2]^{1/2}$$

where $a = \partial N / \partial P$, $b = \partial N / \partial T$, and $c = \partial N / \partial RH$.⁶

Table 2. Minimum specifications for radiosonde sensors.

| Parameter | Precision | Resolution | Range |
|-------------------|-----------|------------|----------------|
| Temperature | 0.5°C | 0.1°C | -10 to 40°C |
| Relative humidity | 5% | 1% | 20 to 100% |
| Pressure | 3 mb | 0.5 mb | 850 to 1050 mb |

The two main types of instruments that can be used to obtain refractivity profiles of the boundary layer are the radiosonde and the refractometer. Environmental measurements using the refractometer, while practical, are neither simple nor inexpensive. If used, the refractometer should have a precision of ± 2 *N*-units.

Radiosondes are commonly borne aloft by balloons. Radiosondes packaged to be launched from an aircraft (dropsondes) are also available. In recent years, the technology for launching a radiosonde package with a small rocket has been developed; the rocket boosts the package to a given altitude, where it is ejected to descend by parachute as it makes measurements.

Balloon-borne radiosondes are relatively inexpensive at a cost of approximately \$100 (U.S.) per launch for sonde, balloon, and gas. Ground-station equipment is considerably more expensive, depending upon the features of the equipment. This equipment may be available for lease. Radiosondes carried aloft by an aerostat, under the control of a winch, are also an option. Detailed sounding procedures will be specified in manufacturer's instructions. Procedures applicable to NAAWS include selecting an appropriate site (or sites) for launch and handling that minimizes spurious sensor readings. Spurious sensor readings can arise from radiative and conductive heating from surrounding structures or from failing to acclimatize the radiosonde to ambient conditions after removing it from a heated or air-conditioned space.

Aboard a boat or ship, the radiosonde should be launched from as low an altitude as possible on the windward side of the bow or stern in order to minimize the heat island effect of the ship. Care should be taken to acclimatize the sonde to ambient conditions before releasing it; that is, the sensors should be given at least 15 seconds to adjust to the outside conditions before launch. Similar procedures are appropriate for launch sites on coastal structures.

If the radiosonde is launched from shore, the launch site should be as close to the water as possible, and precautions should be taken to minimize radiative and conductive heating effects from parking lots, buildings, and other structures. Near active airways, coordination with air control personnel may be required.

If the wind at the time of the radiosonde observation is such that the air has had a long overwater trajectory (>100 km), the boundary layer should be representative of open-ocean conditions. The assumption of horizontal homogeneity usually will be valid, and one sounding will generally be representative of conditions over the path of interest to NAAWS. However, if the wind is offshore or alongshore, propagation conditions over the propagation path are likely to be inhomogeneous, and a minimum of two soundings should be taken along the path within one-half hour of each other.

Balloon ascent rates should be in the range of 200 to 300 m/min. Slower ascent rates yield a higher vertical resolution in the data but may not provide adequate ventilation of the sensors. Faster ascent rates provide good sensor ventilation, but some vertical resolution is lost.

All data collected during the sounding, whether digital or analog, should be retained. Sounding systems that provide automatic data analysis use criteria for selecting significant data that are oriented toward fulfilling meteorological data requirements; these criteria may be too lenient for detailed propagation assessment.

4.0 SURFACE MEASUREMENTS

4.1 SURFACE LAYER

The atmospheric surface layer is usually dominated by mechanical and buoyant turbulence. The average profile of wind, temperature, humidity, or any conservative scalar is determined by the turbulent motions. Roll presents an overview of the wind, temperature, and moisture fields in the first few meters above the sea surface.⁷ Direct measurements of the profiles in the surface layer over the ocean are quite difficult and essentially impractical on an operational basis. To circumvent this difficulty, semiempirical relationships between the profiles and the fluxes of momentum, heat, and moisture have been developed.

4.1.1 Refractive Structure

In meteorology, it is convenient to work with parameters which are invariant with height in homogeneous air.⁴ These are often referred to as potential parameters and conservative properties with respect to adiabatic processes. For radio propagation, the profile of potential refractivity is of interest, with potential refractivity defined by

$$N_p = \frac{77.6 P_o}{\theta} + 3.73 \times 10^5 \frac{e_p}{\theta^2}$$

where $P_o = 1000$ mb, θ is potential temperature in Kelvin, and e_p is potential vapor pressure in millibars. Further

$$\theta = T \left(\frac{P_o}{P} \right)^{0.286}$$

and

$$e_p = e \left(\frac{P_o}{P} \right)$$

where T is temperature in Kelvin, P is pressure in millibars, and e is water vapor pressure in millibars. Over the ocean, the profile of potential refractivity is usually such that trapping gradients exist in the first few meters of the surface layer, and a shallow duct, called the evaporation duct because of the predominant influence of evaporation in causing the trapping gradient, is found. The parameter that best characterizes propagation is the evaporation duct height, defined as the height at which the gradient of potential refractivity reaches the critical value, calculated by ray theory, which will cause a ray launched horizontally to have a curvature exactly equal to the curvature of the earth. In terms of modified refractivity, M , the evaporation duct height is the height in the surface layer at which the M profile reaches its minimum value and the M -gradient is zero. Figure 3 shows an example of an M profile.

There are several semiempirical techniques to relate surface profiles to meteorological measurements that can be simply made at sea. Jeske examined several schemes and correlated evaporation duct height to propagation measurements.⁸⁻¹⁰ His work is the basis for the duct height formulation that follows; this formulation is developed in more detail in Appendixes A, B, and C. A FORTRAN 77 program and test case calculations are provided

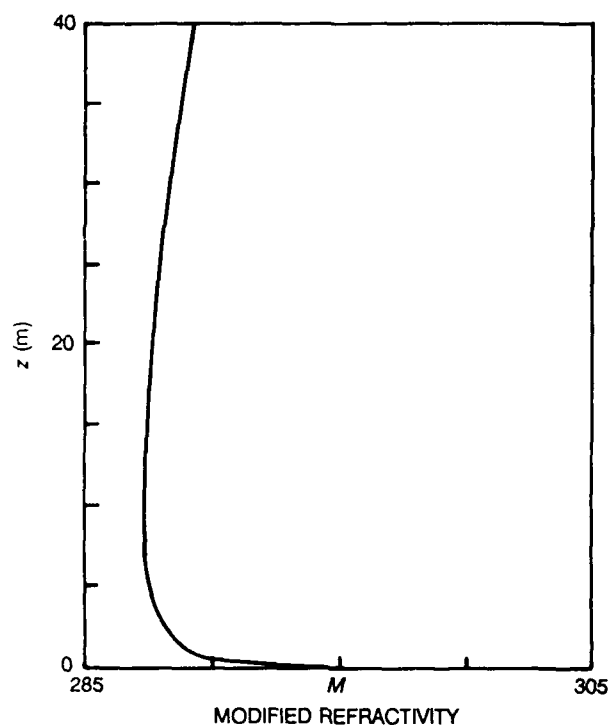


Figure 3. Example of a modified refractivity profile for a 10-m evaporation duct. At the surface, $M = 300$; z is altitude.

in Appendixes D and E, respectively. Appendix F develops the equations for the M -profile in terms of duct height and stability for use in propagation models. Rotherham has developed a similar formulation in a slightly different manner.¹¹

The following six steps specify the calculation of the evaporation duct height:

1. The four bulk meteorological measurements required are air temperature, T_a , and sea temperature, T_s , in Celsius; relative humidity, RH , in percent; and wind speed, u , in knots. Temperatures are converted to Kelvin by $T_{ak} = T_a + 273.2$ and $T_{sk} = T_s + 273.2$. If the wind speed is less than 0.01 knot, the evaporation duct height is set to 0 meters.

2. The bulk Richardson number is calculated by

$$Ri_h = 369 z_1 (T_a - T_s) / (T_{ak} u^2)$$

where z_1 is the reference altitude in meters. Ri_h is restricted to be no greater than 1.

3. Assuming that, in the surface layer, $T_{ak} \approx \theta$, $e \approx e_p$, and neglecting the effect of salinity on vapor pressure, calculate potential refractivity for the air, N_A , at height z_1 and for the air immediately in contact with the sea surface, N_S :

$$N_A = \frac{77.6}{T_{ak}} \left(1000 + \frac{4810}{T_{ak}} e \right)$$

$$N_S = \frac{77.6}{T_{sk}} \left(1000 + \frac{4810}{T_{sk}} e_0 \right)$$

where the ambient vapor pressure of the air, e , is calculated by

$$e = \frac{RH}{100} e_s$$

with

$$e_s = 6.105 \exp \left(25.22 \frac{T_{ak} - 273.2}{T_{ak}} - 5.31 \ln \frac{T_{ak}}{273.2} \right)$$

and the vapor pressure at the sea surface, e_0 , is

$$e_0 = 6.105 \exp \left(25.22 \frac{T_{sk} - 273.2}{T_{sk}} - 5.31 \ln \frac{T_{sk}}{273.2} \right)$$

4. For thermally neutral and stable conditions ($0 \leq Ri_b \leq 1$), the evaporation duct height, δ , is calculated by

$$(a) \quad \delta = 0 \text{ for } \Delta N_p \geq 0$$

or

$$(b) \quad \delta = \frac{\Delta N_p}{b_1 B - \Delta N_p \alpha / L'}$$

or, if the result of (b) is such that $\delta < 0$ or $\delta / L' > 1$, then

$$(c) \quad \delta = \frac{\Delta N_p (1 + \alpha) - b_1 \alpha z_1}{b_1 \ln(z_1 / z_0)}$$

For stable conditions, the function B is

$$B = \ln \left(\frac{z_1}{z_0} \right) + \frac{\alpha z_1}{L'}$$

5. For thermally unstable conditions ($Ri_b < 0$), evaporation duct height, δ , is calculated by

$$\delta = \left[\left(\frac{b_1 B}{\Delta N_p} \right)^4 - \frac{4 \beta}{L'} \left(\frac{b_1 B}{\Delta N_p} \right)^3 \right]^{-1/4}$$

and the function, B , is

$$B = \ln \left(\frac{z_1}{z_0} \right) - \psi$$

The universal function, ψ , is determined by

$$\psi = -4.5 \frac{z_1}{L'} \quad \frac{z_1}{L'} \geq -0.01$$

$$\psi = 10^{[1.02 \log(-z_1/L') + 0.69]} \quad -0.01 > \frac{z_1}{L'} \geq -0.026$$

$$\psi = 10^{[0.776 \log(-z_1/L') + 0.306]} \quad -0.026 > \frac{z_1}{L'} \geq -0.1$$

$$\psi = 10^{[0.630 \log(-z_1/L') + 0.16]} \quad -0.1 > \frac{z_1}{L'} \geq -1$$

$$\psi = 10^{[0.414 \log(-z_1/L') + 0.16]} \quad -1 > \frac{z_1}{L'} \geq -2.2$$

$$\psi = 2 \quad \frac{z_1}{L'} < -2.2$$

6. The maximum value of evaporation duct height is limited to 40 meters. Remaining variables and constants are defined as follows:

$\Delta N_p = N_A - N_S$, potential refractivity difference between the air and the sea

$z_1 = 6$ meters, reference altitude

$b_1 = -0.125 \text{ m}^{-1}$, critical gradient of potential refractivity

$z_0 = 1.5 \times 10^{-4} \text{ m}$, surface roughness parameter

$\beta = 4.5$, coefficient in the unstable function

$\alpha = 5.2$, coefficient in the stable function

$L' = \frac{10 z_1 \Gamma_e}{Ri_b} \text{ m}$, Monin-Obukhov length, where

$$\Gamma_e = 0.05$$

$$Ri_b \leq -3.75$$

$$\Gamma_e = 0.065 + 0.004 Ri_b$$

$$-3.75 < Ri_b \leq -0.12$$

$$\Gamma_e = 0.109 + 0.367 Ri_b$$

$$-0.12 < Ri_b \leq 0.14$$

$$\Gamma_e = 0.155 + 0.021 Ri_b$$

$$0.14 < Ri_b$$

The dominant factor in determining evaporation duct height is the difference in potential refractivity between the air at the reference altitude and the air at the sea surface. Errors in air temperature measurement caused by conductive and radiative heating effects have been shown to strongly affect the duct height calculation.¹² To minimize the sensitivity of the evaporation duct algorithm, an additional test is applied whenever $T_a - T_s > -1$. Evaporation duct height is calculated for $T_a = T_s$, (δ_0), and for $T_a = T_s - 1$, (δ_1), with T_s , u , and RH unchanged. Then, if $\delta_0 > \delta_1$, the value of δ_1 is the evaporation duct height; otherwise, the evaporation duct height is calculated as defined in steps 1 through 6 above.

4.1.2 Measurements and Procedures

The bulk meteorological measurements required for the evaporation duct calculation are wind speed, air and sea temperature, relative humidity, and altitude of the measurements. Since gradients in the surface layer generally become small at altitudes more than a few meters, the influence of measurement altitude is neglected as long as measurements are made at least 6 meters above the surface. Additionally, the influence of sea waves on the measurements is usually restricted to altitudes less than three times the wave height (Ref. 7, p. 123, and Ref. 13), and the altitude of 6 meters or greater minimizes most wave effects.

4.1.2.1 Wind Speed

Wind speed can be measured with the typical cup or aerovane anemometer. The anemometer should be mounted so as to minimize the disturbance to the air flow caused by the observing platform. On a ship or a boat, the anemometer should be mounted as far forward and as high as possible; the measured relative wind must be corrected for ship's course and speed to determine true wind. On piers or other coastal structures, the anemometer should be mounted so it faces into the prevailing wind and is at least 2 meters above the top of the structure. Hand-held anemometers can also be used successfully if carried to the windward side of the platform.

The wind speed should be averaged over a period of 5 to 10 minutes. This will average out the turbulent fluctuations in wind speed. Figure 4 is an overwater power spectrum of wind; a frequency of 2×10^{-3} to 3×10^{-3} Hz represents an averaging period over approximately 5 to 10 minutes and avoids the turbulent peak at 0.01 Hz.¹⁴⁻¹⁵

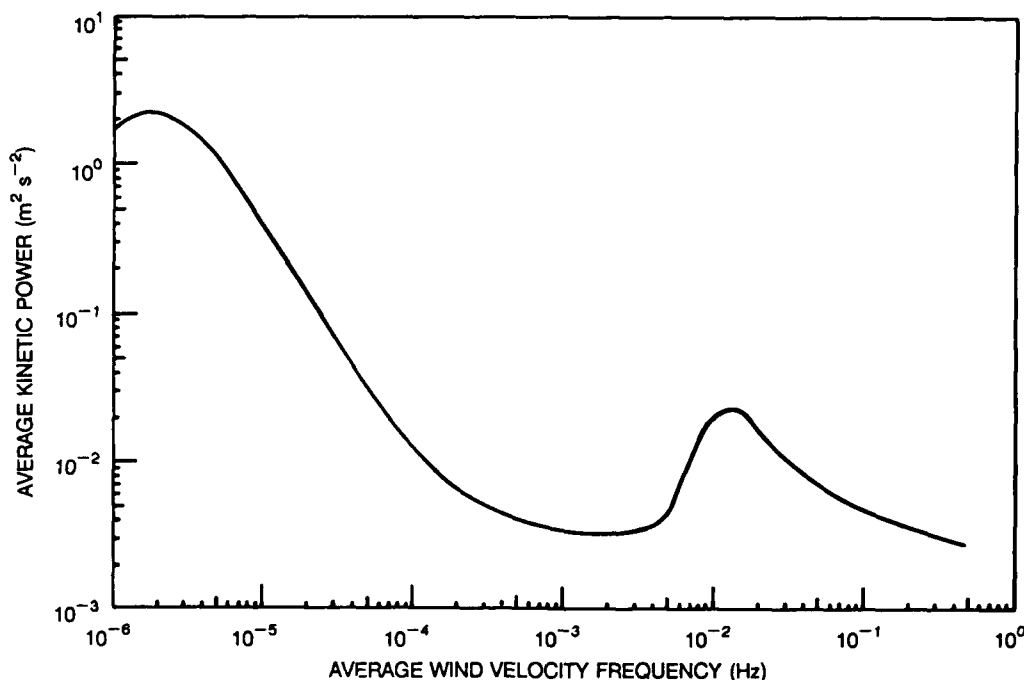


Figure 4. Byshev and Ivanov¹⁴ composite average wind velocity power spectrum for the marine atmospheric surface layer from data taken over the South Atlantic. (From Ref.15.)

4.1.2.2 Air Temperature and Relative Humidity

Measurement of air temperature and relative humidity can be made at any well-exposed site above an altitude of 6 meters with reasonable precautions taken to minimize platform-induced conductive and radiative heating. An aspirated psychrometer with wet and dry bulb thermometers is a convenient portable instrument. Thermometers or other types of temperature and humidity probes can be installed in a thermal screen mounted in a location exposed to the ambient air. Temperature and moisture have spectral properties similar to those shown in Fig. 4.¹⁶ However, since temperature and humidity gradients above 6 meters in the typical overwater surface layer are quite small, averaging times for these parameters can be 3 to 5 minutes.

4.1.2.3 Sea Surface Temperature

The simplest measurement of sea surface temperature is made with a small rubber bucket (or any container with a small thermal mass) and an accurate thermometer. More durable, specifically designed water thermometer buckets are available which provide a frame for a thermometer and a small reservoir (bucket) to retain water around the thermometer bulb. These devices are used to sample the water over a finite depth (~ 0.3 meter). Under most conditions, the wind is sufficient to mix the upper levels of the water column (>2 meters). However, on cloudless days with strong solar heating and light winds, the surface temperature can vary considerably from the underlying water. In these instances, care must be taken to get a representative sample in the upper 0.3 meter of the sea.

Infrared radiometer sensors provide a remote means to sense the sea surface temperature. Although considerably more expensive than the buckets, they do have the advantage of sensing only the sea surface. If this sort of instrument is used, it should have a means to compensate for reflected sky radiation.

Further information on instruments and procedures can be found in Ref. 7, 15, and 17-19. Table 3 shows the minimum specifications for surface measurements.

Table 3. Minimum specifications for surface measurements.

| Parameter | Precision | Range |
|-------------------|-------------------------|-----------------------------------|
| Wind direction | ± 5 deg | 5 to 360 deg |
| Wind speed | ± 2 kt | 0 to 30 kt |
| Air temperature | $\pm 0.5^\circ\text{C}$ | -10° to 40°C |
| Relative humidity | $\pm 5\%$ | 0 to 100% |
| Sea temperature | $\pm 0.5^\circ\text{C}$ | -1° to 40°C |
| Wave height | ± 0.5 m | 0 to 6 m |

4.2 OCEAN WAVES

The state of the sea affects the sea clutter return for radar systems. The disturbance of the sea surface varies in scale from ripples through short-crested (wind) waves to long-wavelength swells. Ripples (capillary waves) are the immediate response of the sea surface to the wind stress. Short-crested waves develop as the average wind continues to exert a stress on the sea surface. If the wind acts over a large enough area (fetch) for a sufficient

period of time (duration), a steady-state condition is reached (fully-arisen sea). Swells are long-wavelength periodic waves formed by the dispersion of wind waves as they propagate away from the area of generation. The local sea state is determined by the superposition of the locally generated ripples and wind waves and the swell propagating through from distant (possibly multiple) sources. Wind-wave height is well-correlated to the average wind speed in the open ocean. Nearby land masses or major ocean currents (e. g., Gulf Stream) may affect this correlation by creating lower or higher wave heights.

To quantify the sea conditions for sea-clutter modeling, it is necessary to measure wind speed, as discussed above, wind direction, and significant wave height. Significant wave height is defined as the average of the highest one-third of the waves and is correlated to what a careful observer would visually judge as the predominant wave height.^{20, 21} The best way to estimate the significant wave height is by observing the variation of the height of the sea surface against a ship's freeboard or a coastal structure's piling. More precise estimates can be made by analyzing wave recorder records or buoy data if available.

Wind direction can be measured by a wind vane as part of a wind measuring system or estimated by an observer. Wind direction, like wind speed, should be averaged over 5 to 10 minutes. Relative wind direction determined aboard a moving ship must be corrected for ship's course and speed.

Table 3 includes minimum specifications for ocean wave measurements.

5.0 EQUIPMENT REFERENCES

The following sample listing of some manufacturers and retailers is provided as possible sources for various types of instruments and equipment. This listing is not all-inclusive nor is it intended to be an endorsement of those companies or products.

- Atmospheric Instrumentation Research Inc., 8401 Baseline Road A, Boulder, CO 80303: USA: radiosonde systems, aerostats.
- Belfort Instrument Company, 727 South Wolfe Street, Baltimore, MD 21231: USA: meteorological instruments.
- Everest Interscience Inc., 1120 South Raymond Avenue, Fullerton, CA 92631: USA: infrared thermometers.
- Kahlsico International Corporation, P.O. Box 947, El Cajon, CA 92022: USA: meteorological and oceanographic equipment; water bucket thermometer.
- Qualimetrics Inc., P.O. Box 41039, Sacramento, CA 95841, Representatives Science Associates, P.O. Box 230, Princeton, NJ 08542, and Qualimetrics LTD, % Gold Crest, Prospect Business Center, Dundee Technology Park, Unit No. 24, Dundee, Scotland DD21TY, U.K.: radiosonde systems and meteorological instruments.
- Rotronic Instrument Corporation, 7 High Street, Huntington, NY 11743: USA: meteorological probes.
- Vaisala Oy, PL 26, SF-00421, Helsinki 42, Finland, with subsidiaries Vaisala Inc., 2 Tower Office Park, Woburn, MA 01801 and Vaisala (UK) LTD, 11 Billing Road, Northampton NN1 5AW, U.K.: radiosonde systems and surface meteorological instruments.
- VIZ Manufacturing Company, 335 East Price Street, Philadelphia, PA 19144-5782 USA: radiosonde systems.

6.0 GLOSSARY

The semantics of the various terms that are used in describing the performance of instruments necessitates defining the terms as they are used in this document. These definitions follow Brock.¹⁸

accuracy — used in this document only as a general, descriptive term of an instrument's performance.

lag — the time difference between when a specific value of output is obtained and when that same value was previously obtained by the input.

precision — a statistical description of the amount of deviation from the most likely value for the measured quantity.

range — the interval of the measured quantity over which the instrument is designed to be sensitive.

resolution — the smallest variation in the input that causes a detectable change in the output.

7.0 REFERENCES

1. Hitney, H.V., "Evaporation Duct Effects on Low-Altitude Propagation: Guidelines for the NATO AAW System Project," Naval Ocean Systems Center TD 1304, June 1988.
2. Reilly, J.P., "Clutter Models for Shipboard Radar Application: 0.5 to 70 GHz," John Hopkins Univ./ Applied Physics Laboratory F2A-88-0-307R/NAAW-88-062R, June 1988.
3. Davidson, K.L., G.E. Schacher, C.W. Fairall, P. Jones Boyle, and D.A. Brower, "Marine Atmospheric Boundary Layer Modeling for Tactical Use," Naval Postgraduate School NPS-63-82-001, Sep 1982.
4. Craig, R.A., I. Katz, R.B. Montgomery, and P.J. Rubenstein, "Meteorology of the Refraction Problem," in *Propagation of Short Radio Waves*, D.E. Kerr, ed., New York, McGraw-Hill, pp. 181-293, 1951.
5. Helvey, R.A., "Radiosonde Errors and Spurious Surface-Based Ducts," *Proceedings of the Institute of Electrical Engineers*, Part F, 130(7), 643-648, 1983.
6. Paulus, R.A., "Data Quality in EM Propagation Models," in *Proceedings of the Conference of Microwave Propagation in the Marine Boundary Layer*, Naval Environmental Prediction Research Facility TR 89-02, Jan 1989.
7. Roll, H.U., *Physics of the Marine Atmosphere*, International Geophysics Series, vol. 7, New York, Academic Press, 1965.
8. Jeske, H., "Die Ausbreitung elektromagnetischer Wellen im cm- bis m-Band über dem Meer unter besonderer Berücksichtigung der meteorologischen Bedingungen in der maritimen Grenzschicht," *Hamburger Geophysikalische Einzelschriften*, De Gruyter, Hamburg, 1965.
9. _____ "The State of Radar-Range Prediction over Sea," in *Tropospheric Radio Wave Propagation, Part II*, NATO-AGARD Conference Proceedings No. 70, Feb 1971.
10. _____ "State and Limits of Prediction Methods of Radar Wave Propagation Conditions over Sea," in *Modern Topics in Microwave Propagation and Air-Sea Interaction*, A. Zancla, ed., Reidel Pub., 1973.
11. Rotheram, S., "Radiowave Propagation in the Evaporation Duct," *The Marconi Review*, 37(192), pp. 18-40, 1974.
12. Paulus, R.A., "Practical application of an evaporation duct model," *Radio Science*, vol. 20, no. 4, pp. 887-896, 1985.
13. Krügermeyer, L., M. Grünwald, and M. Dunkel, "The influence of sea waves on the wind profile," *Boundary Layer Meteorology*, vol. 14, pp. 403-414, 1978.
14. Byshev, V.I., and Y.A. Ivanov, "The time spectra of some characteristics of the atmosphere above the ocean," *Izv. Acad. Sci. USSR, Atmos. Oceanic Phys.*, vol. 5, pp. 8-13, 1969 [English translation].
15. Blanc, T.V., "A Practical Approach to Flux Measurements of Long Duration in the Marine Atmospheric Surface Layer," *Journal of Climate and Applied Meteorology*, vol. 22, pp. 1093-1110, 1983.
16. Panofsky, H.A., and J.A. Dutton, *Atmospheric Turbulence*, New York, John Wiley & Sons, p. 87, 1984.

17. Dobson, F. I., Hasse, and R. Davis, eds., *Air-Sea Interaction Instruments and Methods*, New York, Plenum Press, 1980.
18. Brock, F.V., ed., *Instructor's Handbook on Meteorological Instrumentation*, NCAR Technical Note 237+IA, National Center for Atmospheric Research, Boulder, CO, 1984.
19. Meteorological Office, *Handbook of Meteorological Instruments*, London, Her Majesty's Stationery Office, 1981.
20. Sverdrup, H.W., M.W. Johnson, and R.H. Fleming, *The Oceans*, Englewood Cliffs, Prentice-Hall, pp. 533-534, 1942.
21. Pierson, W.J., Jr., G. Neumann, and R.W. James, *Observing and Forecasting Ocean Waves*, U.S. Navy Hydrographic Office Pub. No. 603, Washington, DC, U.S. Naval Oceanographic Office, p. 16, 1955.

Appendix A

DEVELOPMENT OF THE EVAPORATION DUCT HEIGHT FORMULATION

References A-1 to A-3 provide a detailed development of the evaporation duct height formulation by Jeske. A general development of Jeske's formulation is included here along with assumptions and rationale for the implementation in the computer program listing in Appendix D.

Jeske defined the gradient

$$\frac{\partial \iota}{\partial z} = \frac{S_{\iota}}{\rho \kappa u_* (z + z_0)} \phi \quad (\text{A-1})$$

where ι is a scalar property of the atmosphere, S_{ι} is the vertical flux of ι , z is height in meters, κ is von Karmen's constant (0.4), u_* is the friction velocity in m/s, z_0 is the roughness parameter in meters, and ϕ is a stability-dependent function (equal to 1 at thermally neutral conditions, i. e., air temperature equal to sea surface temperature). For stable conditions (air warmer than water), the stability function was taken to be the logarithmic-linear model proposed by Monin and Obukhov:

$$\phi\left(\frac{z}{L'}\right) = 1 + \alpha \frac{z}{L'} \quad (\text{A-2})$$

where α is taken to be 5.2 and L' is the gradient form of the Monin-Obukhov scaling length corrected for stability. For unstable conditions (water warmer than air), the KEYPS relationship

$$\phi^4 - 4 \alpha \frac{z}{L'} \phi^3 = 1 \quad (\text{A-3})$$

with $\alpha = 4.5$ is used. To evaluate z/L' , the bulk Richardson number is used as

$$Ri_b = \frac{g \Delta T z}{T u^2 \Gamma} \quad (\text{A-4})$$

where $g = 9.8 \text{ m/s}^2$, z is height in meters, T is air temperature in Kelvin, ΔT is air temperature minus sea temperature, u is wind speed in m/s, and Γ is the profile coefficient. Ri_b involves approximating gradients with differences and assumes $T \approx \theta$ in the surface layer. The profile coefficient for neutral conditions is

$$\Gamma = \frac{1}{\ln\left(\frac{z_1 + z_0}{z_0}\right)} \quad (\text{A-5})$$

and is approximately 0.1 for typical observation heights, z_1 , and surface roughness parameter values, z_0 , of 0.00015 meter. Similarly, L' is

$$L' = \frac{T u^2 \Gamma_e}{g \Delta T} \quad (\text{A-6})$$

or, in terms of Ri_b ,

$$\frac{1}{L'} = \frac{Ri_b}{10 z_1 \Gamma_e} \quad (\text{A-7})$$

where Γ_e is an empirical profile coefficient for nonneutral conditions (Fig. A-1). Γ_e is evaluated by a straight-line-segment fit to the data in Fig. A-1.

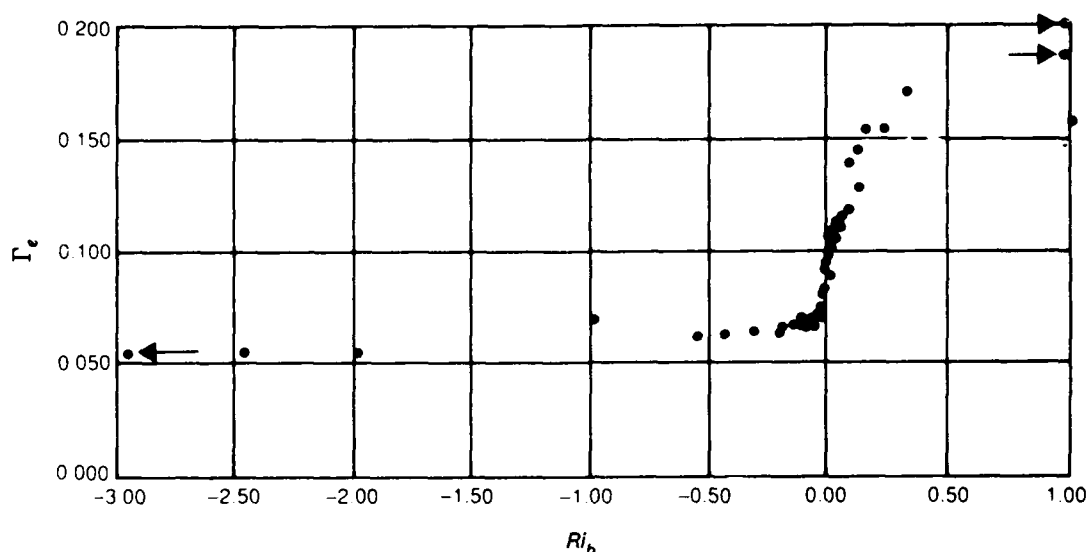


Figure A-1. The profile coefficient, Γ_e , as a function of bulk Richardson number, Ri_b . (From Jeske.^{A-1 to A-3})

Returning to Eq. A-1, assume the flux, S_t , is constant with height and integrate from the sea surface to z_1 :

$$\iota_1 - \iota_0 = \Delta \iota_1 = \frac{S_t}{\rho \kappa u_*} \int_0^{z_1} \frac{\phi}{z + z_0} dz \quad (\text{A-8})$$

Thus, the flux term is

$$\frac{S_t}{\rho \kappa u_*} = \frac{\Delta \iota_1}{\int_0^{z_1} \frac{\phi}{z + z_0} dz} \quad (\text{A-9})$$

and substituting in Eq. A-1 yields

$$\frac{\partial \iota}{\partial z} = \frac{\Delta \iota \phi}{B (z + z_0)} \quad (\text{A-10})$$

where

$$B = \int_0^{z_1} \frac{\phi}{z + z_0} dz \quad (\text{A-11})$$

Taking the scalar ι as potential refractivity, N_p , the height, δ , at which the critical gradient of potential refractivity, $b_1 = -0.125 \text{ m}^{-1}$, occurs is found from Eq. A-10 as

$$\delta = \frac{\Delta N_p}{b_1 B - \Delta N_p \alpha / L'} \quad (\text{A-12})$$

where ϕ for stable conditions is determined from Eq. A-2 and B is evaluated as

$$B = \ln \frac{z_1}{z_0} + \frac{\alpha}{L'} z_1 \quad (\text{A-13})$$

Jeske recommends that δ/L' should not exceed 1. If this occurs, then duct height should be recalculated with $\delta/L' = 1$.

For unstable conditions, solving Eq. A-10 for ϕ in terms of N_p , substituting in Eq. A-3 with $z = \delta$, and solving yields

$$\delta = \left[\left(\frac{b_1 B}{\Delta N_p} \right)^4 - \frac{4 \alpha}{L'} \left(\frac{b_1 B}{\Delta N_p} \right)^3 \right]^{1/4} \quad (\text{A-14})$$

where B is evaluated as

$$B = \ln \frac{z_1}{z_0} - \psi \left(\frac{z_1}{L'} \right) \quad (\text{A-15})$$

$\psi(z_1/L')$ has the analytic form^{A-4}

$$\psi = 1 - \phi - 3 \ln \phi + 2 \ln \left(\frac{1 + \phi}{2} \right) + 2 \tan^{-1} \phi - \frac{\pi}{2} + \ln \left(\frac{1 + \phi^2}{2} \right) \quad (\text{A-16})$$

Use of Eq. A-16 requires the iterative solution of Eq. A-3 for ϕ with a given z/L' . ψ can be more quickly determined by a straight-line-segment fit to the KEYPS profile of Fig. A-2 adapted from Lumley and Panofsky.^{A-5}

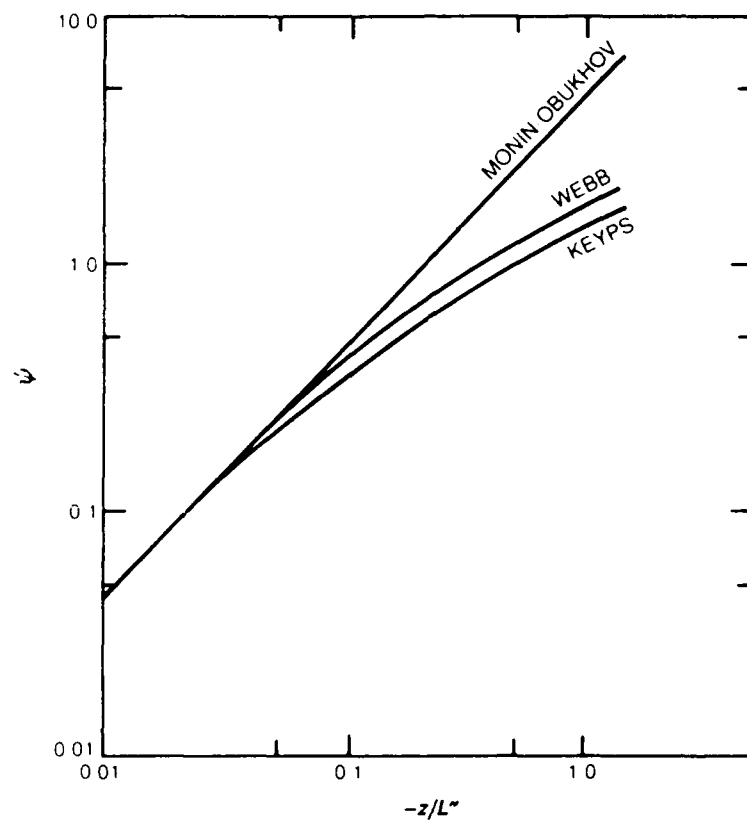


Figure A-2. Universal function ψ as a function of z/L^* . (From Lumley and Panofsky.^{A-5})

REFERENCES FOR APPENDIX A

- A-1. Jeske, H., "Die Ausbreitung elektromagnetischer Wellen im cm- bis m-Band über dem Meer unter besonderer Berücksichtigung der meteorologischen Bedingungen in der maritimen Grenzschicht," *Hamburger Geophysikalische Einzelschriften*, De Gruyter, Hamburg, 1965.
- A-2. _____, "The State of Radar-Range Prediction over Sea," in *Tropospheric Radio Wave Propagation, Part II*, NATO-AGARD Conference Proceedings No. 70, Feb 1971.
- A-3. _____, "State and Limits of Prediction Methods of Radar Wave Propagation Conditions over Sea," in *Modern Topics in Microwave Propagation and Air-Sea Interaction*, A. Zancla, ed., Reidel Pub., 1973.
- A-4. Paulson, C. A., "The Mathematical Representation of Wind Speed and Temperature Profiles in the Unstable Atmospheric Surface Layer," *Journal of Applied Meteorology*, vol. 9, pp. 857-861, Dec 1970.
- A-5. Lumley, J.L., and H.A. Panofsky, *The Structure of Atmospheric Turbulence*, New York, Interscience Publishers, p. 113, 1964.

Appendix B

CRITICAL GRADIENT OF POTENTIAL REFRACTIVITY

The equation for refractivity in terms of pressure, P , in millibars, temperature, T , in Kelvin, and water vapor pressure, e , in millibars is

$$N = \frac{77.6 P}{T} + 3.73 \times 10^5 \frac{e}{T^2} \quad (\text{B-1})$$

For application in the atmospheric surface layer, potential refractivity

$$N_p = \frac{77.6 P_o}{\theta} + 3.73 \times 10^5 \frac{e_p}{\theta^2} \quad (\text{B-2})$$

is the conservative property where P_o is a reference pressure level (taken to be 1000 mb), θ is potential temperature, and e_p is potential water vapor pressure.

From geometric optics, the critical gradient required for trapping is that which yields a ray curvature equal to the earth's curvature

$$\frac{dN}{dz} = -\frac{10^6}{a} = -0.157 \text{ N/m} \quad (\text{B-3})$$

where a is the earth's radius, 6371×10^3 m. To relate the gradient of potential refractivity to the gradient of refractivity, take the total derivatives of $N_p(\theta, e_p)$ and $N(P, T, e)$ with respect to z . Assuming $\theta \approx T$ and $e_p \approx e$ in the surface layer yields

$$\frac{dN_p}{dz} = \frac{dN}{dz} - \frac{\partial N}{\partial P} \frac{dP}{dz} \quad (\text{B-4})$$

The partial derivative $\partial N / \partial P = 77.6 / T$ varies from 0.28 to 0.26 mb^{-1} over the temperature range of 0° to 30°C. The derivative dP/dz can be evaluated by making the hydrostatic approximation

$$\frac{dP}{dz} = -\rho g = -\frac{P g}{R T} \quad (\text{B-5})$$

where ρ is density, g is acceleration of gravity (9.8 m/s^2), P is pressure (1000 mb), R is the individual gas constant for dry air ($2.87 \times 10^6 \text{ erg/g/}^\circ\text{K}$), and T is temperature ($^\circ\text{K}$). This yields a variation of dP/dz from -0.12 to -0.11 mb/m over the temperature range of 0° to 30°C. Taking standard temperature (15°C), the critical gradient for trapping, in terms of potential refractivity, is

$$\frac{dN_p}{dz} = -0.157 - (0.27)(-0.12) = -0.125 \text{ m}^{-1} \quad (\text{B-6})$$

Appendix C

IMPLEMENTING A MODIFIED EVAPORATION DUCT HEIGHT CALCULATION

Reference C-1 showed that a bias in air-sea temperature difference toward thermal stability resulted in spuriously high calculated evaporation duct heights. A modification to the duct height calculation that detected and compensated for the air-sea temperature difference bias was proposed based on the variation of duct height as a function of air-sea temperature difference at a constant relative humidity. To implement the algorithm, the value of either the air temperature or sea temperature may have to be changed to yield a modified air-sea temperature difference. A comparison of climatological air and sea temperatures from Marsden square data^{C-2} and ocean data buoys^{C-3} showed better agreement between sea temperature means than between air temperature means. Air temperature means from the Marsden square data also indicate a diurnal variation ($\sim 1^\circ\text{C}$) that the buoy data do not show. Mean air temperatures for 3-hour intervals for data buoys show diurnal variations of only a few tenths of a degree.* This gives more weight to holding sea temperature constant and varying air temperature to obtain the appropriate air-sea temperature difference.

The next question that arises, then, is whether or not it is reasonable to hold relative humidity constant while changing air temperature. Reed reported finding systematic errors in air temperature measurements aboard a ship but did not find systematic errors in relative humidity measurements.^{C-4} Experience with psychrometric measurements in a thermal screen during the Ku-Band Surface Surveillance Project^{C-5} sited on Point Loma in San Diego tends to support Reed's findings. Recommendations of a working group on the computation of global air-sea flux climatology to use both daytime and nighttime humidities but only nighttime air and sea temperature lend support to the assumption of negligible bias in the relative humidity measurements.^{C-6}

The implementation of the modified evaporation duct height calculation assumes that air temperature can be varied to obtain the appropriate air-sea temperature differences while sea temperature, wind speed, and relative humidity are held constant. Figure C-1 is a flow chart of the process.

*D.B. Gilhousen, National Oceanic and Atmospheric Administration Data Buoy Center, personal communication, January 1984.

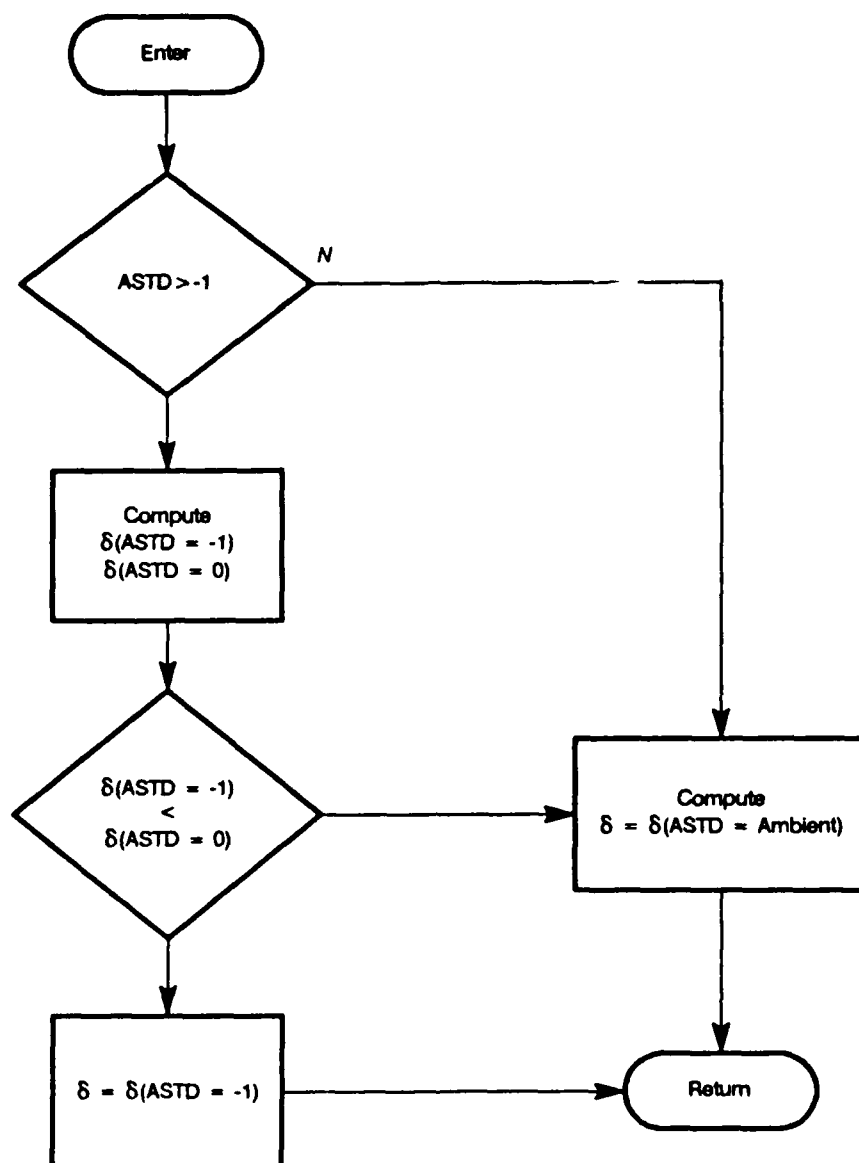


Figure C-1. Flow chart for the modified evaporation duct calculation based on air – sea temperature difference (ASTD).

REFERENCES FOR APPENDIX C

- C-1. Paulus, R.A., "Practical Application of the IREPS Evaporation Duct Model," Naval Ocean Systems Center TR 966, June 1984.
- C-2. Naval Oceanography Command Detachment Asheville, "Evaporation Duct Report 76118," June 1981.
- C-3. National Climatic Data Center, "Climatic Summaries for NOAA Data Buoys," Jan 1983.
- C-4. Reed, R.K., "An Example of Shipboard Air Temperature Errors," *Mariner's Weather Log*, vol. 22, no. 1, pp. 13-14, Jan 1978.
- C-5. Anderson, K.D., "Radar Measurements at 16.5 GHz in the Oceanic Evaporation Duct," *IEEE Transactions on Antennas and Propagation*, vol. 37, no. 1, pp. 100-106, Jan 1989.
- C-6. Scoggins, J.R., and C.N.K. Mooers, "Workshop on Atmospheric Forcing of Ocean Circulation," *Bulletin American Meteorological Society*, vol. 69, no. 11, p. 1349-1353, Nov 1988.

Appendix D

FORTTRAN PROGRAM TO CALCULATE EVAPORATION DUCT HEIGHT

```
c
c      *****
c
c      name:      delta.f
c
c      routine controls the execution of the 'get_delta'
c      function for testing the calculations of the evaporation
c      duct height (delta).
c
c      language: fortran iv ('77)
c      machine:  hp 520 (unix)
c
c      call sequence:
c              MAIN routine
c
c      glossary:
c          airt:      air temperature, deg C
c          seat:      sea temperature, deg C
c          rh:        relative humidity, %
c          u:         wind speed, knots
c
c      subroutines:
c          get_delta (function)
c          evap
c
c      rev      date      description
c      0.00     101987
c
c      *****
c      prompt the user for entries, call 'get_delta' to
c      compute the evaporation duct height
c      *****
c
c      write(*,9000)
9000  format( "Compute the evaporation duct height from"/
*      "entries of:"/
*      " air temperature, deg C"/
*      " sea temperature, deg C"/
*      " relative humidity, % and"/
*      " wind speed, knots"/)
c
c      write(7,9010)
9010  format("..air...|.sea...|.rh...|...u...|.delta.|"/
*      " temp   | temp   | %    | knots | meters")
c
c      do while(.true.)
c
c          write(*,'("enter air temp (C): ",$)')
```

```

    read(*,*) airt
    write(*,('enter sea temp (C): ",$)')
    read(*,*) seat
    write(*,('enter relative humidity (%): ",$)')
    read(*,*) rh
    write(*,('enter wind speed (knots): ",$)')
    read(*,*) u
    delta=get_delta(airt, seat, rh, u)
    write(7,9010)
    write(7,9020) airt,seat,rh,u,delta
9020    format(5f8.1)
enddo
end

```



```

c
c *****
c
c   name:      get_delta.f
c
c   routine calculates the evaporation duct height using
c   the paulus formulation "Practical Application of the
c   IREPS Evaporation Duct Model", NOSC TR 966, Jun 84
c
c   language:  fortran iv ('77)
c   machine:   hp 520 (unix)
c
c   call sequence:
c       delta=get_delta(airt, seat, rh, u)
c
c   glossary:
c       airt:      air temperature, deg C
c       seat:      sea temperature, deg C
c       rh:        relative humidity, %
c       u:         wind speed, knots
c
c   subroutines:
c       evap
c
c   rev      date      description
c   0.00    101987      modify 'duct63' program code to
c                   make a stand-alone utility.
c
c *****
c
c   function  get_delta(airt,seat,rh,u)
c
c *****
c
c   check wind speed, convert to deg K, and compute
c   vapor pressures
c
c   if (u .gt. .01) then
c
c       wvel=u
c
c       dtok=273.2
c
c       tak=airt+dtok
c       tsk=seat+dtok
c
c       esw=6.105*exp(25.22*seat/tsk-5.31*alog(tsk/dtok))
c       es =6.105*exp(25.22*airt/tak-5.31*alog(tak/dtok))
c       e  =rh*es/100.
c
c   calculate delta
c
c       t1=tsk-1.0          !modified air temp

```

```

        if(tak .gt. t1) then
            el=rh*esw/100.
            call evap(wvel,tsk,tsk,el,esw,del0)
            esl=6.105*exp(25.22*(seat-1.0)/t1-5.31*alog(t1/dtok))
            el=rh*esl/100.
            call evap(wvel,t1,tsk,el,esw,delta)
            if(del0-delta .lt. 0.) then
                call evap(wvel,tak,tsk,e,esw,delta)
            endif
        else
            call evap(wvel,tak,tsk,e,esw,delta)
        endif

    else

        delta=0.

    end if

    get_delta=amin1(delta,40.)

    return

end

```

```

c *****
c
c Name:    EVAP
c
c Routine calculates the evaporation duct height
c (in metres) following the method of Jeske "The State
c of Radar Range Prediction over Sea", Tropospheric
c Radio Wave Propagation - Part II, NATO-AGARD, Feb 71
c
c Language:  FORTRAN IV ('77)
c Machine :  Univac 1100/82
c
c      CALL Evap(wvel,tak,tsk,e,esw,delta)
c
c      wvel:   Wind speed knots
c      tak:    Air temperature in Kelvin
c      tsk :   Sea temperature in Kelvin
c      e :     Vapor pressure mbs
c      esw :   Surface vapor pressure mbs
c      delta   Duct height m RETURNED
c
c      Rev    Date      Description
c      0.0    052984
c *****
c
c      subroutine evap(wvel,tak,tsk,e,esw,delta)
c
c      real lnz1z0
c
c      -----
c
c      delta=0.           !default duct height
c      z0=1.5e-4          !roughness height
c      z1=6.              !reference height (m)
c      beta=4.5           !constant
c      alpha=5.2          !constant
c      lnz1z0=log(z1/z0)  !useful
c      b1=-0.125          !potential refractivity trapping grad.
c
c      -----
c
c      rib=369.*z1*(tak-tsk)/(tak*wvel*wvel)
c      if(rib .gt. 1.) rib=1.
c
c      compute potential refractivity difference
c
c      delna=77.6/tak*(1000.+4810.*e/tak)
c      deln0=77.6/tsk*(1000.+4810.*esw/tsk)
c      deln=delna-deln0
c      if(deln .ge. 0.) return
c
c      -----
c      compute the gamma function

```

```

c      if(rib .le. -3.75) then
c          gamma=0.05
c      else if(rib .le. -0.12) then
c          gamma=0.065+rib*0.004
c      else if(rib .le. 0.14) then
c          gamma=0.109+rib*0.367
c      else
c          gamma=0.155+rib*0.021
c      end if

c      olp=rib/(10.*z1*gamma)          !1./L'
c      zlolp=z1*olp

c      -----
c      compute Psi function for unstable conditions
c
c      if(rib .lt. 0.) then
c          if(zlolp .ge. -0.010) then
c              psi=-4.5*zlolp
c          else if(zlolp .ge. -0.026) then
c              psi=10.**(1.020*alog10(-zlolp)+0.690)
c          else if(zlolp .ge. -0.100) then
c              psi=10.**(0.776*alog10(-zlolp)+0.306)
c          else if(zlolp .ge. -1.000) then
c              psi=10.**(0.630*alog10(-zlolp)+0.160)
c          else if(zlolp .ge. -2.200) then
c              psi=10.**(0.414*alog10(-zlolp)+0.160)
c          else
c              psi=2.000
c          end if

c      Compute unstable delta
c
c          b=lnz1z0-psi
c          btemp=b*b1/deln
c          d=btemp**4 - 4.*beta*olp*btemp**3
c          if(d .gt. 0.) delta=d**(-0.25)

c      Stable and neutral conditions
c
c      else
c          b=lnz1z0+z1olp*alpha
c          delta=deln/(b*b1 - alpha*deln*olp)
c          if(delta .lt. 0. .or. delta*olp .gt. 1.) then
c              delta=(deln*(1.+alpha)-b1*alpha*z1)/(b1*lnz1z0)
c          end if
c      end if

c      Return to caller
c
c      return
c
c      end

```

Appendix E

TEST CASES FOR EVAPORATION DUCT HEIGHT CALCULATION

For the specified inputs of air temperature (°C), sea temperature (°C), relative humidity (%), and wind speed (knots), the evaporation duct height (δ) should be calculated correctly to within ± 0.1 meter.

| Air Temp (°C) | Sea Temp (°C) | RH (%) | <i>u</i> (knots) | δ (m) |
|------------------|------------------|-----------|---------------------|-----------------|
| 0.0 | 15.0 | 10. | 1. | 3.9 |
| 0.0 | 15.0 | 10. | 20. | 16.8 |
| 0.0 | 15.0 | 75. | 1. | 2.8 |
| 0.0 | 15.0 | 75. | 20. | 12.3 |
| 0.0 | 15.0 | 100. | 1. | 2.4 |
| 0.0 | 15.0 | 100. | 20. | 10.4 |
| 0.0 | 16.0 | 10. | 1. | 4.0 |
| 0.0 | 16.0 | 10. | 20. | 17.3 |
| 0.0 | 16.0 | 75. | 1. | 3.0 |
| 0.0 | 16.0 | 75. | 20. | 13.0 |
| 0.0 | 16.0 | 100. | 1. | 2.6 |
| 0.0 | 16.0 | 100. | 20. | 11.2 |
| 15.0 | 15.0 | 10. | 1. | 8.7 |
| 15.0 | 15.0 | 10. | 20. | 37.0 |
| 15.0 | 15.0 | 75. | 1. | 3.6 |
| 15.0 | 15.0 | 75. | 20. | 13.9 |
| 15.0 | 15.0 | 100. | 1. | 0.0 |
| 15.0 | 15.0 | 100. | 20. | 0.0 |
| 15.0 | 16.0 | 10. | 1. | 9.1 |
| 15.0 | 16.0 | 10. | 20. | 38.8 |
| 15.0 | 16.0 | 75. | 0 | 0.0 |
| 15.0 | 16.0 | 75. | 1. | 3.8 |
| 15.0 | 16.0 | 75. | 20. | 14.6 |
| 15.0 | 16.0 | 100. | 1. | 0.9 |
| 15.0 | 16.0 | 100. | 20. | 2.6 |
| 30.0 | 15.0 | 10. | 1. | 8.7 |
| 30.0 | 15.0 | 10. | 20. | 37.0 |
| 30.0 | 15.0 | 75. | 1. | 3.6 |
| 30.0 | 15.0 | 75. | 20. | 13.9 |
| 30.0 | 15.0 | 100. | 1. | 0.0 |

(Cont'd)

| Air Temp (°C) | Sea Temp (°C) | <i>RH</i> (%) | <i>u</i> (knots) | δ (m) |
|------------------|------------------|------------------|---------------------|-----------------|
| 30.0 | 15.0 | 100. | 20. | 0.0 |
| 30.0 | 16.0 | 10. | 1. | 9.1 |
| 30.0 | 16.0 | 10. | 20. | 38.8 |
| 30.0 | 16.0 | 75. | 1. | 3.8 |
| 30.0 | 16.0 | 75. | 20. | 14.6 |
| 30.0 | 16.0 | 100. | 1. | 0.0 |
| 30.0 | 16.0 | 100. | 20. | 0.0 |

Appendix F

M-PROFILES IN THE SURFACE LAYER

Propagation models require a refractivity profile to make their calculations. The procedures specified in the main text yield only a scalar duct height. In a manner similar to Jeske,* an equation for M versus height can be developed. The equation for potential refractivity, N_p , is

$$N_p = \frac{77.6 P_o}{\theta} + 3.73 \times 10^5 \frac{e_p}{\theta^2} \quad (\text{F-1})$$

where P_o is a reference pressure (1000 mb), θ is potential temperature ($^{\circ}\text{K}$), and e_p is potential water vapor pressure (mb). The total derivative of N_p with respect to altitude, z , is

$$\frac{dN_p}{dz} = \frac{\partial N_p}{\partial \theta} \frac{d\theta}{dz} + \frac{\partial N_p}{\partial e_p} \frac{de_p}{dz} \quad (\text{F-2})$$

The partial derivatives in Eq. F-2 are evaluated as

$$\frac{\partial N_p}{\partial \theta} = - \frac{77.6 P_o}{\theta^2} - 7.46 \times 10^5 \frac{e_p}{\theta^3} \quad (\text{F-3})$$

$$\frac{\partial N_p}{\partial e_p} = \frac{3.73 \times 10^5}{\theta^2}$$

Over the range of 0° to 30°C , $\partial N_p / \partial \theta$ varies from -1.2 to $-1.6 / ^{\circ}\text{K}$; $\partial N_p / \partial e_p$ varies from 5.0 to $4.1 / \text{mb}$ (for potential vapor pressure equal to 80% of saturation). Then, for 15°C and 80% relative humidity, Eq. F-2 becomes

$$\frac{dN_p}{dz} = - 1.4 \frac{d\theta}{dz} + 4.5 \frac{de_p}{dz} \quad (\text{F-4})$$

The potential temperature and potential water vapor profiles in the surface layer are found from

$$\begin{aligned} \frac{d\theta}{dz} &= \frac{\theta_*}{\kappa(z + z_0)} \phi\left(\frac{z}{L'}\right) \\ \frac{de_p}{dz} &= \frac{e_{p*}}{\kappa(z + z_0)} \phi\left(\frac{z}{L'}\right) \end{aligned} \quad (\text{F-5})$$

*Jeske, H., "State and Limits of Prediction Methods of Radar Wave Propagation Conditions over Sea," in *Modern Topics in Microwave Propagation and Air-Sea Interaction*, A. Zanca, ed., Reidel Pub., 1973.

where θ_* and e_{p*} are scaling quantities, κ is von Karmen's constant, z is altitude, z_0 is the aerodynamic roughness parameter, L' is the Monin-Obukhov scaling length corrected for stability, and $\phi(z/L')$ is a stability-dependent function. Equation F-4 then becomes

$$\frac{dN_p}{dz} = -1.4 \frac{\theta_*}{\kappa(z + z_0)} \phi\left(\frac{z}{L'}\right) + 4.5 \frac{e_{p*}}{\kappa(z + z_0)} \phi\left(\frac{z}{L'}\right) \quad (\text{F-6})$$

The scaling quantities for a given set of conditions are determined from bulk meteorological measurements

$$\theta_* = \kappa \frac{\theta(z_1) - \theta(z_0)}{\ln\left(\frac{z_1 + z_0}{z_0}\right) - \psi\left(\frac{z_1}{L'}\right)} \quad (\text{F-7})$$

$$e_{p*} = \kappa \frac{e_p(z_1) - e_p(z_0)}{\ln\left(\frac{z_1 + z_0}{z_0}\right) - \psi\left(\frac{z_1}{L'}\right)}$$

where z_1 is the reference altitude and $\psi(z_1/L')$ is the integrated stability-dependent function. Substitution of Eq. F-7 into Eq. F-6 yields

$$\frac{dN_p}{dz} = \frac{\phi\left(\frac{z}{L'}\right)}{(z + z_0)} \frac{\Delta N_p}{\ln\left(\frac{z_1 + z_0}{z_0}\right) - \psi\left(\frac{z_1}{L'}\right)} \quad (\text{F-8})$$

where ΔN_p is the bulk air-sea potential refractivity difference

$$\Delta N_p = -1.4 [\theta(z_1) - \theta(z_0)] + 4.5 [e_p(z_1) - e_p(z_0)] \quad (\text{F-9})$$

The evaporation duct height, δ , is the height at which the gradient of potential refractivity is -0.125 m^{-1} . Thus Eq. F-8 becomes

$$-0.125 = \frac{\phi\left(\frac{\delta}{L'}\right)}{(\delta + z_0)} \frac{\Delta N_p}{\ln\left(\frac{z_1 + z_0}{z_0}\right) - \psi\left(\frac{z_1}{L'}\right)} \quad (\text{F-10})$$

Solving Eq. F-10 for ΔN_p and substituting into Eq. F-8 gives

$$\frac{dN_p}{dz} = -0.125 \frac{(\delta + z_0)}{\phi\left(\frac{\delta}{L'}\right)} \frac{\phi\left(\frac{z}{L'}\right)}{(z + z_0)} \quad (\text{F-11})$$

But, $dN_p/dz = dM/dz - 0.125$, and the M -gradient is

$$\frac{dM}{dz} = 0.125 - 0.125 \frac{(\delta + z_0)}{\phi\left(\frac{\delta}{L'}\right)} \frac{\phi\left(\frac{z}{L'}\right)}{(z + z_0)} \quad (\text{F-12})$$

Integrating

$$M(z) = M_o + 0.125 z - 0.125 \frac{\delta + z_0}{\phi\left(\frac{\delta}{L'}\right)} \int_0^z \frac{\phi\left(\frac{z}{L'}\right)}{z + z_0} dz \quad (\text{F-13})$$

For stable conditions, the stability-dependent function has the form, $\phi = 1 + \alpha z/L'$, and Eq. F-13 becomes

$$M(z) = M_o + 0.125 z - 0.125 \frac{\delta}{1 + \frac{\alpha\delta}{L'}} \left(\ln \frac{z + z_0}{z_0} + \frac{\alpha z}{L'} \right) \quad (\text{F-14})$$

where z_0 has been neglected relative to δ . For unstable conditions, the stability-dependent function has the form,

$$\phi^4 - 4\alpha \frac{z}{L'} \phi^3 = 1$$

and Eq. F-13 becomes

$$M(z) = M_o + 0.125 z - 0.125 \frac{\delta}{\phi\left(\frac{\delta}{L'}\right)} \left[\ln \frac{z + z_0}{z_0} - \psi\left(\frac{z}{L'}\right) \right] \quad (\text{F-15})$$

where z_0 has again been neglected relative to δ . ϕ and ψ can be determined as in Appendix A. It has been found through numerous propagation experiments and model simulations that the neutral M -profile is a good representation of practical evaporation duct conditions. For neutral conditions, $\phi = 1$ and $\psi = 0$, and Eq. F-15 is simply

$$M(z) = M_o + 0.125 z - 0.125 \delta \ln \frac{z + z_0}{z_0} \quad (\text{F-16})$$

The aerodynamic roughness parameter, z_0 , is taken to be constant at 1.5×10^{-4} meter.

REPORT DOCUMENTATION PAGEForm Approved
OMB No. 0704-0188

Public reporting burden for this collection of information is estimated to average 1 hour per response, including the time for reviewing instructions, searching existing data sources, gathering and maintaining the data needed, and completing and reviewing the collection of information. Send comments regarding this burden estimate or any other aspect of this collection of information, including suggestions for reducing this burden, to Washington Headquarters Services, Directorate for Information Operations and Reports, 1215 Jefferson Davis Highway, Suite 1204, Arlington, VA 22202-4302, and to the Office of Management and Budget, Paperwork Reduction Project (0704-0188), Washington, DC 20503.

| | | | | | |
|---|---|--|----------------------------|--|--|
| 1. AGENCY USE ONLY (Leave blank) | | 2. REPORT DATE November 1989 | | 3. REPORT TYPE AND DATES COVERED Final: Oct 1988—Oct 1989 | |
| 4. TITLE AND SUBTITLE SPECIFICATION FOR ENVIRONMENTAL MEASUREMENTS TO ASSESS RADAR SENSORS | | | | 5. FUNDING NUMBERS 63790N, R1962, DN 888 715 | |
| 6. AUTHOR(S) Richard A. Paulus | | | | | |
| 7. PERFORMING ORGANIZATION NAME(S) AND ADDRESS(ES) Naval Ocean Systems Center San Diego, CA 92152-5000 | | | | 8. PERFORMING ORGANIZATION REPORT NUMBER NOSC TD 1685 | |
| 9. SPONSORING/MONITORING AGENCY NAME(S) AND ADDRESS(ES) Naval Sea Systems Command U. S. Short Range AAW Project Office Code 06APN Washington, DC 20363 | | | | 10. SPONSORING/MONITORING AGENCY REPORT NUMBER | |
| 11. SUPPLEMENTARY NOTES | | | | | |
| 12a. DISTRIBUTION/AVAILABILITY STATEMENT Approved for public release; distribution is unlimited. | | | | 12b. DISTRIBUTION CODE | |
| 13. ABSTRACT (Maximum 200 words) The minimum requirements are described for the measurement of environmental parameters that will affect the evaluation of proposed radar systems developed for the NATO Anti-Air Warfare System Project. General procedures are given for making short-term meteorological measurements relevant to radar propagation and sea clutter. Several types of instruments capable of making these measurements are described. | | | | | |
| 14. SUBJECT TERMS environmental measurements refraction ducting evaporation duct | | | | 15. NUMBER OF PAGES 43 | |
| | | | | 16. PRICE CODE | |
| 17. SECURITY CLASSIFICATION OF REPORT UNCLASSIFIED | 18. SECURITY CLASSIFICATION OF THIS PAGE UNCLASSIFIED | 19. SECURITY CLASSIFICATION OF ABSTRACT UNCLASSIFIED | 20. LIMITATION OF ABSTRACT | | |